Invited Paper

Plasmon-exciton coupling between silver nanowire and two quantum dots

Qiang Li[a], Hong Wei*[a], and Hongxing Xu[a,b]

[a]Institute of Physics, Chinese Academy of Sciences, and Beijing National Laboratory for Condensed Matter Physics, Beijing 100190, China
[b]Center for Nanoscience and Nanotechnology, and School of Physics and Technology, Wuhan University, Wuhan 430072, China

*weihong@iphy.ac.cn

ABSTRACT

We report the first experimental demonstration of plasmon-exciton coupling between silver nanowire (NW) and a pair of quantum dots (QDs). The resolving of single surface plasmons (SPs) generated in the NW-QD pair system is achieved. The accurate positions of the two QDs and NW ends are obtained by using a maximum likelihood single molecule localization method, and the separation distances between the two QDs range from microns to 200 nm within the diffraction limit. Parameters including the SP propagation length and the wire terminal reflectivity are experimentally determined and taken into account. The efficiency of plasmon generation due to the exciton-plasmon coupling is obtained for each QD.

Keywords: Quantum dot, silver nanowire, surface plasmons, super-resolution imaging, single photon source

1. INTRODUCTION

The interaction between quantum emitters and photons is one of the most important research directions of quantum information science and the key of the realization of quantum switch, quantum logic gate, quantum storage and so on. Plasmonic waveguide, which offers enhanced local electromagnetic field and propagating surface plasmons (SPs), presents us a new method to control the light-matter interaction at the nanometer scale[1-5]. Chemically synthesized crystalline metal nanowires (NWs) can support propagating SPs with lower losses than lithographically defined waveguides and can be easily manipulated to construct complex optical devices, which make them ideal candidates to enhance the light-matter interaction at the nanometer scale[6-14].

Quantum dot (QD) is a widely accepted candidate for single photon source with tunable emission spectra, which can be a key component for the quantum information technology[15-17]. In 2007, plasmon-exciton coupling in a system of Ag NW and single QD was demonstrated by Akimov et al[18]. Inspired by this experimental work, a novel scheme that can generate quantum entangled states in a system of two quantum emitters positioned near a plasmonic waveguide is proposed and investigated theoretically[19-23]. Here we report the first experimental demonstration of plasmon-exciton coupling between silver NW and two QDs. The separation between the two QDs we studied is ranging from microns to 200 nm within the diffraction limit. The SP-generation efficiency of each QD is derived.

2. SAMPLE PREPARATION

The Ag NWs synthesized using solution-phase polyol methods[24] were deposited onto glass slides cleaned by the piranha solution and dried naturally. The slides with Ag NWs were immediately covered by Al_2O_3 of 10 nm thickness using atomic layer deposition method (Cambridge NanoTech, Savannah-100). Then CdSe/ZnS QDs (Qdot® 655 ITK™, Invitrogen) were spin coated onto the sample. Finally copper grids with marked number were stuck onto the slides, which can help to find the same NW with both an optical microscope and a scanning electron microscope (SEM). A typical SEM image of Ag NWs we used is shown in Figure 1a. Figure 1b shows the histogram of wire diameter for 70 wires. A transmission electron microscopy (TEM) image of the QDs is shown in Figure 1c.

Plasmonics: Metallic Nanostructures and Their Optical Properties XII, edited by Allan D. Boardman, Proc. of SPIE Vol. 9163, 91630Z · © 2014 SPIE
CCC code: 0277-786X/14/$18 · doi: 10.1117/12.2061519

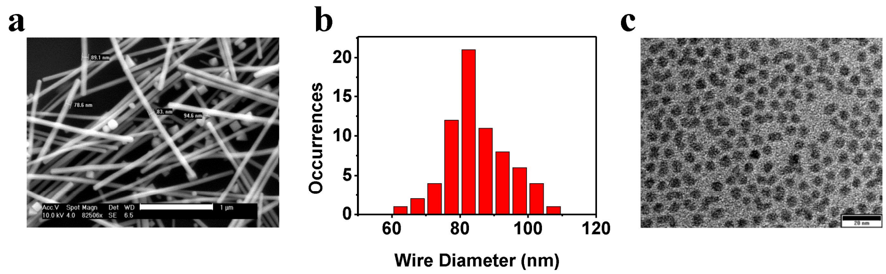

Figure 1. (a, b) SEM image of Ag NWs and histogram of wire diameter distribution. The scale bar in (a) is 1 μm. (c) TEM image of the QDs. The scale bar is 20 nm.

3. EXPERIMENTAL SETUP

Our optical setup is based on an inverted microscope. As shown in Figure 2, laser light of 532 nm wavelength was focused onto the sample from the glass side using a 100× oil immersion objective (NA 1.4, Olympus). The fluorescence from the QDs was collected by the same objective and detected by an electron multiplying charge-coupled device (EMCCD) (iXon DV887, Andor) operating at frame rate of 10 or 20 Hz. To measure the fluorescence lifetime and second-order correlation function, the fluorescence is guided to two confocal detection paths that enable light detection from an area as small as 1 μm in diameter on the sample surface and detected by two single photon avalanche diodes (SPAD) (PDM, Micro Photon Devices). The recorded signals are analyzed using a time-correlated single photon counting module (PicoHarp300, PicoQuant).

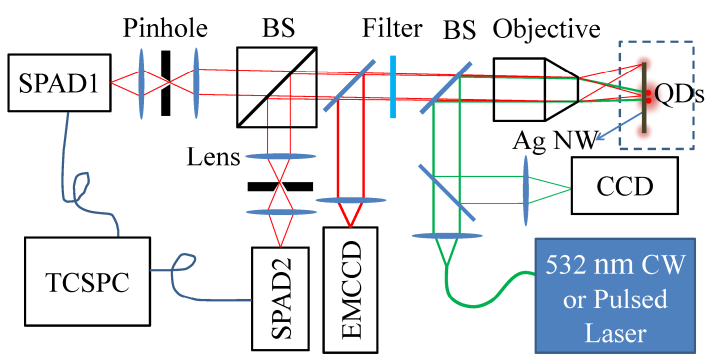

Figure 2. Schematic illustration of the optical setup. BS is a beam splitter. SPAD1 and SPAD2 are two single photon avalanche diodes. TCSPC means a time-correlated single photon counting module.

4. RESULT AND DISCUSSION

4.1 QD pair with large separation coupled with a Ag NW

Figure 3a shows the photoluminescence (PL) image of a NW-QD pair system, where the separation between the two QDs is about 2 μm. In order to realize the simultaneous excitation of the two QDs A and B, we added a lens into the optical path to expand the excitation spot to a size of about 4 μm in diameter. The bright spots marked as A and B are from the direct photon emission of the excited QD pair. The photons at spots C and D are from the NW end scattering of the propagating SPs generated by the two QDs[18, 25-28]. Time traces of fluorescence counts (integrated over the pixels in the light pink squares in Figure 3a) from the QDs A and B show a blinking behavior, that is, the emission is randomly switched between ON (bright) and OFF (dark) states under continuous excitation, which is a character of single quantum dot[29, 30]. The blinking curves of the scattered photons at C and D show two-level "ON" states, which indicates that both QDs A and B are efficiently coupled with the NW and they both contribute to the generation of propagating SPs.

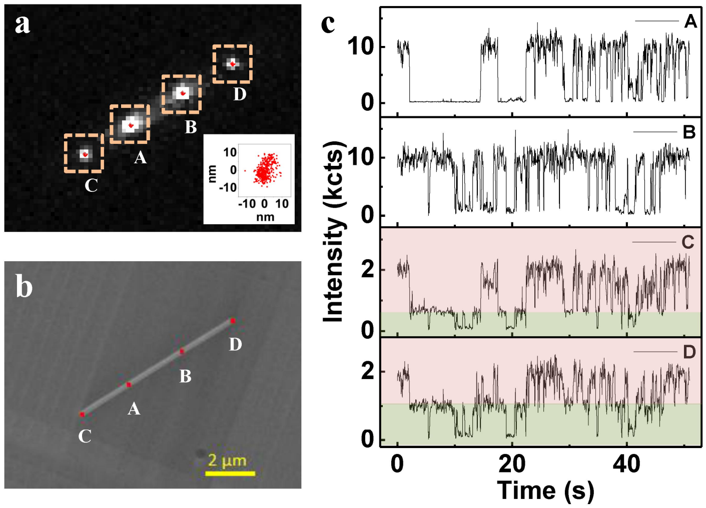

Figure 3. Ag NW coupling with simultaneously excited QD pair. (a) PL image shows the coupling of two QDs with the Ag NW. The measured positions of QDs A and B, NW terminals C and D are labeled with red stars. The inset shows the enlarged view of the measured positions of QD A. (b) SEM image of the same NW. The measured positions of QDs and NW ends are overlaid. (c) Time traces of fluorescence counts of QDs A and B, and scattered light at the NW ends C and D. The two bright states of the fluorescence counts at C and D are denoted with two different color areas. The intensity unit kcts means 1000 counts. The light pink squares in (a) show the regions where the counts of each pixel are integrated to generate the emission counts.

Figure 4 shows the fluorescence decay histograms for QDs A and B coupled to the NW and for an uncoupled reference QD on substrate. For the uncoupled QD on substrate, a single exponential fit yields an excited state lifetime of about 24.2 ns. As a consequence of coupling with the NW, the QDs A and B get additional recombination channels[31], resulting in a reduced excited state lifetime of 5.6 ns and 7.7 ns, respectively.

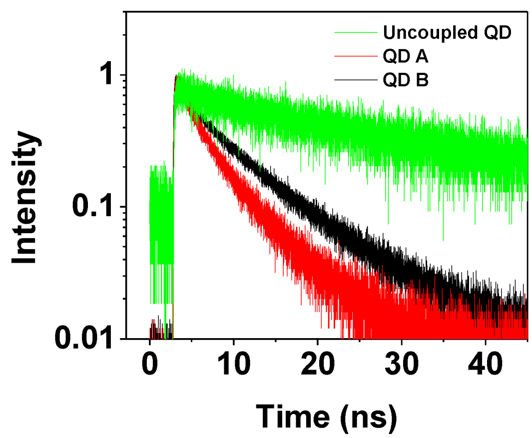

Figure 4. PL decay curves of an uncoupled reference QD (green line), coupled QD A (red line) and QD B (black line).

In order to quantitatively characterize the coupling strength between QD and Ag NW, we define the SP-generation efficiency as the percentage of the QD energy converted to guided SPs. This value can be expressed as follows (here the

QD energy does not include the part damped non-radiatively and the collection efficiency of our detection system for the NW end emission and QD emission is assumed to be equal):

$$\eta = \frac{I_{End1}e^{\beta L_{QD-End1}} + I_{End2}e^{\beta L_{QD-End2}}}{I_{QD}\delta + I_{End1}e^{\beta L_{QD-End1}} + I_{End2}e^{\beta L_{QD-End2}}} \tag{1}$$

Here η is the SP-generation efficiency, I_{End1} and I_{End2} are the intensity of the scattered light at the two ends of the NW, I_{QD} is the direct photon emission intensity of the QD, $1/\beta$ is the propagation length of SPs, $L_{QD-End1}$ and $L_{QD-End2}$ are the distances between the QD and the two NW ends, δ is the transmittance of the NW ends, which is experimentally obtained as 0.68[32]. On the basis of the assumption that the probability of the energy from the QD converting to SPs propagating on the NW in two opposite directions is equal, the scattering counts at C and D can be expressed as a superposition of the emission counts of the two QDs A and B with different weight dependent on both the QD positions and their SP-generation efficiency:

$$\begin{aligned} I_C &= \frac{1}{2}I_A\delta\exp\left(-\beta L_{A-C}\right)\frac{\eta_A}{1-\eta_A} + \frac{1}{2}I_B\delta\exp\left(-\beta L_{B-C}\right)\frac{\eta_B}{1-\eta_B} \\ I_D &= \frac{1}{2}I_A\delta\exp\left(-\beta L_{A-D}\right)\frac{\eta_A}{1-\eta_A} + \frac{1}{2}I_B\delta\exp\left(-\beta L_{B-D}\right)\frac{\eta_B}{1-\eta_B} \end{aligned} \tag{2}$$

Here the accurate distances between the two QDs and NW ends can be obtained by using a maximum likelihood single molecule localization method[33-36]. The four emission spots A, B, C and D are fitted with two dimensional Gaussian point spread function and the localized centers are labeled with red stars in Figure 3a. The inset of Figure 3a is the enlarged plot of the measured positions of QD A, which presents a spatial resolution of less than 20 nm. Figure 3b shows the SEM image of the NW with the measured positions of QDs and NW ends labeled with red stars. The distances between the emission spots are as follows: L_{A-C} =2064 nm, L_{A-B} = 2338 nm, L_{B-D} = 2204 nm. On the basis of the time traces of fluorescence counts at A and B, we used three free parameters η_A, η_B and β to fit the time trace recorded at terminal C. The fitting result is $\eta_A = 0.39$, $\eta_B = 0.31$ and $1/\beta = 4634$ nm.

In order to study the exciton-plasmon coupling independently, we used a focused laser beam to selectively excite each coupled QD (Figure 5). The large spot in Figure 5a corresponds to emission from the QD itself, whereas the two other spots correspond to scattered SPs at the ends of the NW. Figure 5b shows the time trace of the fluorescence counts from the QD A and from the ends of the NW. A high degree of correlation between the blinking curves indicates that the QD A is the source of fluorescence from the wire ends. Measurement results of the second-order correlation function of the NW-QD A coupling system are shown in Figure 5c, where A and C represent detectors aligned to the emission spots at A and C in Figure 5a. Both second-order correlation function of A&A and A&C show obvious anti-bunching behaviors ($g^{(2)}(0) < 0.5$), which demonstrates the generation of single quantized SPs on the NW[18, 26, 27].

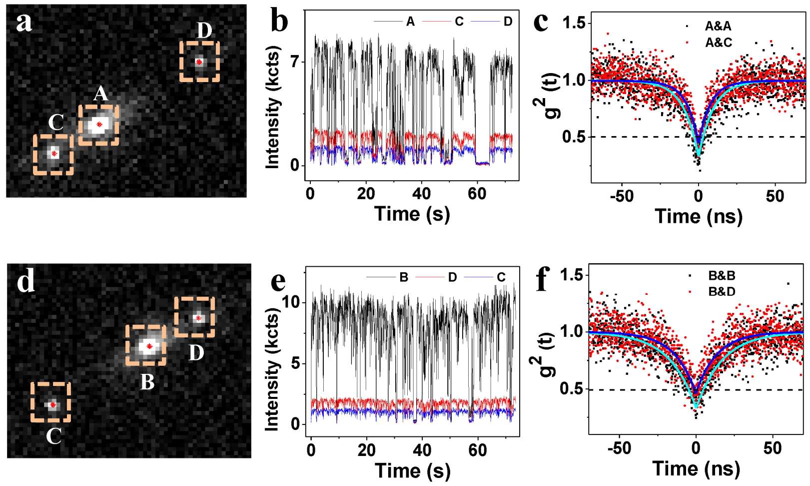

Figure 5. Ag NW coupling with the selectively excited single QD. (a, d) PL image of single QD coupled with a Ag NW. The accurate positions of QD A (B), NW terminals C and D are labeled with red stars. (b, e) Time traces of fluorescence counts of QD A (B) and scattered light at the NW ends C and D. The light pink squares in (a) and (d) show the regions where the counts of each pixel are integrated to generate the emission counts. (c, f) Second-order correlation function $g^{(2)}(t)$ of the NW-QD system. The dots in (c) correspond to the measurements with SPAD1 aligned to emission spot A and SPAD2 to emission spot A (black) or spot C (red) in the PL image shown in (a). The dots in (f) correspond to the measurements with SPAD1 aligned to emission spot B and SPAD2 to emission spot B (black) or spot D (red) in the PL image shown in (d). The cyan (blue) solid lines are exponential fitting of the black (red) dots. The dashed horizontal lines mark the position where $g^{(2)}(t)=0.5$.

The ratio of the counts from both ends I_C/I_D is centered at about 1.77 and this ratio can be related with the propagation length $1/\beta$ using the following equations:

$$\frac{1}{\beta}=\frac{1}{(L_{A-D}-L_{A-C})}\ln(\frac{I_C}{I_D}) \tag{3}$$

A propagation length of 4362 nm is obtained using equation 3. The relationship of emission counts at C and A is as follows:

$$I_C=\frac{1}{2}I_A\delta\exp\left(-\beta L_{A-C}\right)\frac{\eta_A}{1-\eta_A} \tag{4}$$

We use the time trace at A to fit that at C, and obtain the SP-generation efficiency of QD A $\eta_A=0.40$. Using the similar method, we demonstrated the single photon emission of the QD B and the single surface plasmon generation in the NW (Figure 5d-f). The SP-generation efficiency of QD B is $\eta_B=0.32$. The difference of SP-generation efficiency between QD A and QD B might be from the slight difference in the QD-NW separation or QD orientation. The values of SP-generation efficiency and propagation length obtained under both the simultaneous excitation and selective excitation conditions are nearly the same, which indicates that the emission counts at the NW ends result from independent contributions from QDs A and B.

4.2 QD pair within diffraction limit coupled with a Ag NW

Figure 6a shows the PL image of a pair of QDs (separated within the diffraction limit) coupled with a Ag NW, where the two QDs A and B were excited by focused laser beam. The large bright spot and two small light spots correspond to the direct far field emission from the QD pair and scattered SPs at the ends of the NW, respectively. Time traces of fluorescence counts (integrated over the light pink squares shown in Figure 6a) from the QD pair and scattered photons at the ends of the NW are shown in Figure 6c. The two fluorescence "ON" levels correspond to one QD (lower level) and both QDs (upper level) being in the bright state, indicating two QDs being present. Figure 6d (black dots) shows the measured autocorrelation function of the fluorescence from the QD pair ((A & B) & (A & B). The number of QDs in the detection area we estimated through the value of $g^{(2)}(0)$ is two[32, 37, 38]. In order to determine the separation distance between QD A and QD B, we selected the PL images that clearly show only QD A or QD B (pink dots or green dots in Figure 6c) is in the bright state. Then the maximum likelihood single molecule localization method is used to fit the accurate position of the QD. The fitted positions of the QDs and the NW terminals are labeled with red stars in Figure 6a and 6b. The measured separation distance between the two QDs is 217 nm. Using the same method as above, we obtain the propagation length of about 4805 nm through the counts ratio between C and D. The SP-generation efficiencies for the two QDs are deduced from the time traces of emission counts with only QD A or only QD B in the bright state. The result is $\eta_A = 0.33$, $\eta_B = 0.28$. The second-order correlation function between fluorescence of the QD pair and scattering from the NW end C is shown in Figure 6d ((A & B) & C, red dots), which also indicates the emission is from two single photon sources (QDs)[32].

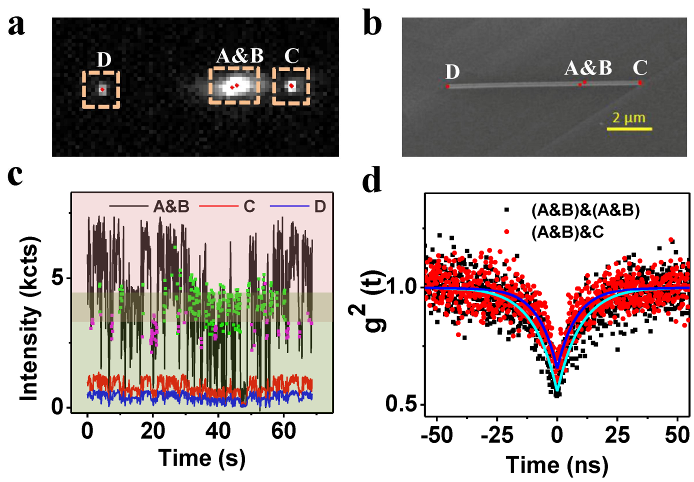

Figure 6. Ag NW coupling with two QDs located in diffraction-limited area. (a) PL image showing the coupling of QDs with the Ag NW. (b) SEM image of the NW. The accurate positions of QDs A and B, and NW terminals C and D are labeled with red stars. (c) Time traces of fluorescence counts of QD pair and scattered light at the NW ends. The pink and green dots correspond to the PL images with only QD A or QD B in the bright state. The pink, grey and cyan areas are used to separate the three bright states. The light pink squares in (a) show the regions where the counts of each pixel are integrated to generate the emission counts. (d) Second-order correlation function $g^{(2)}(t)$ of fluorescence signal for (A&B) & (A&B) (black dots), and (A&B) & C (red dots). The cyan and blue solid lines are exponential fitting results for the black and red dots, respectively.

4.3 Coupling of QD pair with a Ag NW (only one QD coupled with the NW)

In another case of a pair of QDs (distributed within the diffraction limited) in the proximity of a Ag NW, we show that only one QD is coupled with the NW and generates propagating SPs. Figure 7a is the PL image showing the coupling of the QD pair with the Ag NW. The largest bright spot corresponds to the direct fluorescence emission from QDs A and B, while two smaller spots C and D correspond to SPs scattered out at the NW ends. Using the single molecule localization method, the fitted positions of the QDs and the NW terminals are labeled with red stars in Figure 7a and 7b. The measured separation distances of the QD pair is L_{A-B} = 255 nm. Figure 7c shows the time traces of fluorescence counts of the QD pair and scattered SPs at the NW ends C and D. It is found that the traces at C and D are only partly correlated with the time trace of QD pair. The two green boxes mark two clear areas where the counts at C and D are not correlated with the counts of the QD pair, indicating only one QD is coupled with the NW. The fitted positions of the two QDs clearly show that QD B is closer to the NW than QD A, so that only QD B is coupled with the NW and is the energy source of the photons at the NW ends. The SP-generation efficiency for QD B is deduced from the time traces of emission counts with only QD B in the bright state and the result is $\eta_B = 0.57$.

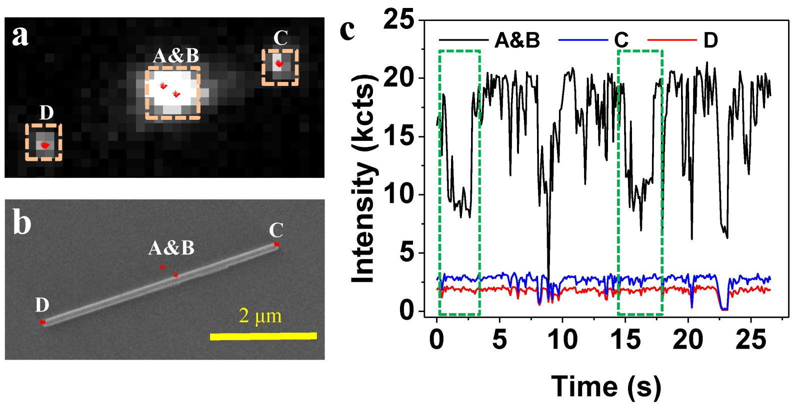

Figure 7. Coupling of QD pair with a Ag NW (only one QD coupled with the NW). (a) PL image showing the coupling of the QD pair with the Ag NW. (b) SEM image of the NW with the measured positions of the QDs and the NW ends overlaid. (c) Time traces of fluorescence counts of QD pair and scattered light at the NW ends C and D.

5. CONCLUSION

In conclusion, we report the careful analysis of exciton-plasmon coupling between a pair of semiconductor QDs and a chemically grown silver NW. By using a super-resolution imaging method, the precise positions of the QDs along the NW are obtained, and the separation between the two QDs in diffraction-limited area is determined. Both the SP propagation length and the wire terminal reflectivity are experimentally obtained. The SP-generation efficiency of the exciton-plasmon coupling is determined for each QD. Our analysis method provides an efficient way to analyze and resolve the coupling of multiple quantum emitters with plasmonic waveguides.

ACKNOWLEDGMENTS

This work was supported by National Natural Science Foundation of China (Grant Nos. 11134013, 11227407 and 11374012), The Ministry of Science and Technology of China (Grant Nos. 2012YQ12006005 and 2009CB930700), the "Knowledge Innovation Project" (Grant No. KJCX2-EW-W04) and the "Strategic Priority Research Program (B)" (Grant No. XDB07030100) of Chinese Academy of Sciences.

REFERENCES

[1] Barnes, W. L., Dereux, A. and Ebbesen, T. W., "Surface plasmon subwavelength optics," Nature 424(6950), 824-830 (2003).

[2] Bozhevolnyi, S. I., Volkov, V. S., Devaux, E., Laluet, J. Y. and Ebbesen, T. W., "Channel plasmon subwavelength waveguide components including interferometers and ring resonators," Nature 440(7083), 508-511 (2006).

[3] Oulton, R. F., Sorger, V. J., Genov, D. A., Pile, D. F. P. and Zhang, X., "A hybrid plasmonic waveguide for subwavelength confinement and long-range propagation," Nat. Photonics 2(8), 496-500 (2008).

[4] Gramotnev, D. K. and Bozhevolnyi, S. I., "Plasmonics beyond the diffraction limit," Nat. Photonics 4(2), 83-91 (2010).

[5] Choo, H., Kim, M. K., Staffaroni, M., Seok, T. J., Bokor, J., Cabrini, S., Schuck, P. J., Wu, M. C. and Yablonovitch, E., "Nanofocusing in a metal-insulator-metal gap plasmon waveguide with a three-dimensional linear taper," Nat. Photonics 6(12), 837-843 (2012).

[6] Ditlbacher, H., Hohenau, A., Wagner, D., Kreibig, U., Rogers, M., Hofer, F., Aussenegg, F. R. and Krenn, J. R., "Silver nanowires as surface plasmon resonators," Phys. Rev. Lett. 95(25), 257403 (2005).
[7] Wei, H., Li, Z. P., Tian, X. R., Wang, Z. X., Cong, F. Z., Liu, N., Zhang, S. P., Nordlander, P., Halas, N. J. and Xu, H. X., "Quantum Dot-Based Local Field Imaging Reveals Plasmon-Based Interferometric Logic in Silver Nanowire Networks," Nano Lett. 11(2), 471-475 (2011).
[8] Wei, H., Wang, Z. X., Tian, X. R., Kall, M. and Xu, H. X., "Cascaded logic gates in nanophotonic plasmon networks," Nat. Commun. 2, 387 (2011).
[9] Wei, H. and Xu, H. X., "Nanowire-based plasmonic waveguides and devices for integrated nanophotonic circuits," Nanophotonics 1(2), 155-169 (2012).
[10] Russell, K. J., Liu, T. L., Cui, S. Y. and Hu, E. L., "Large spontaneous emission enhancement in plasmonic nanocavities," Nat. Photonics 6(7), 459-462 (2012).
[11] Wei, H., Zhang, S. P., Tian, X. R. and Xu, H. X., "Highly tunable propagating surface plasmons on supported silver nanowires," Proc. Natl. Acad. Sci. USA 110(12), 4494-4499 (2013).
[12] Guo, X., Ma, Y. G., Wang, Y. P. and Tong, L. M., "Nanowire plasmonic waveguides, circuits and devices," Laser Photonics Rev. 7(6), 855-881 (2013).
[13] Wu, X. Q., Xiao, Y., Meng, C., Zhang, X. N., Yu, S. L., Wang, Y. P., Yang, C. X., Guo, X., Ning, C. Z. and Tong, L. M., "Hybrid Photon-Plasmon Nanowire Lasers," Nano Lett. 13(11), 5654-5659 (2013).
[14] Pan, D., Wei, H., Jia, Z. L. and Xu, H. X., "Mode Conversion of Propagating Surface Plasmons in Nanophotonic Networks Induced by Structural Symmetry Breaking," Sci. Rep. 4, 4993 (2014).
[15] Ropp, C., Cummins, Z., Nah, S., Fourkas, J. T., Shapiro, B. and Waks, E., "Nanoscale imaging and spontaneous emission control with a single nano-positioned quantum dot," Nat. Commun. 4, 1447 (2013).
[16] Zhang, J. T., Tang, Y., Lee, K. and Ouyang, M., "Tailoring light-matter-spin interactions in colloidal hetero-nanostructures," Nature 466(7302), 91-95 (2010).
[17] Hennessy, K., Badolato, A., Winger, M., Gerace, D., Atature, M., Gulde, S., Falt, S., Hu, E. L. and Imamoglu, A., "Quantum nature of a strongly coupled single quantum dot-cavity system," Nature 445(7130), 896-899 (2007).
[18] Akimov, A. V., Mukherjee, A., Yu, C. L., Chang, D. E., Zibrov, A. S., Hemmer, P. R., Park, H. and Lukin, M. D., "Generation of single optical plasmons in metallic nanowires coupled to quantum dots," Nature 450(7168), 402-406 (2007).
[19] Gonzalez-Tudela, A., Martin-Cano, D., Moreno, E., Martin-Moreno, L., Tejedor, C. and Garcia-Vidal, F. J., "Entanglement of Two Qubits Mediated by One-Dimensional Plasmonic Waveguides," Phys. Rev. Lett. 106(2), 020501 (2011).
[20] Chen, G. Y., Lambert, N., Chou, C. H., Chen, Y. N. and Nori, F., "Surface plasmons in a metal nanowire coupled to colloidal quantum dots: Scattering properties and quantum entanglement," Phys. Rev. B 84(4), 045310 (2011).
[21] Chen, G. Y. and Chen, Y. N., "Correspondence between entanglement and Fano resonance of surface plasmons," Opt. Lett. 37(19), 4023-4025 (2012).
[22] Yang, J., Lin, G. W., Niu, Y. P. and Gong, S. Q., "Quantum entangling gates using the strong coupling between two optical emitters and nanowire surface plasmons," Opt. Express 21(13), 15618 (2013).
[23] Kim, N. C., Li, J. B., Yang, Z. J., Hao, Z. H. and Wang, Q. Q., "Switching of a single propagating plasmon by two quantum dots system," Appl. Phys. Lett. 97(6), 061110 (2010).
[24] Sun, Y. G. and Xia, Y. N., "Large-scale synthesis of uniform silver nanowires through a soft, self-seeding, polyol process," Adv. Mater. 14(11), 833-837 (2002).
[25] Wei, H., Ratchford, D., Li, X. E., Xu, H. X. and Shih, C. K., "Propagating surface plasmon induced photon emission from quantum dots," Nano Lett. 9(12), 4168-4171 (2009).
[26] Kolesov, R., Grotz, B., Balasubramanian, G., Stohr, R. J., Nicolet, A. A. L., Hemmer, P. R., Jelezko, F. and Wrachtrup, J., "Wave-particle duality of single surface plasmon polaritons," Nat. Phys. 5(7), 470-474 (2009).
[27] Huck, A., Kumar, S., Shakoor, A. and Anderson, U. L., "Controlled Coupling of a Single Nitrogen-Vacancy Center to a Silver Nanowire," Phys. Rev. Lett. 106(9), 096801 (2011).
[28] Li, Q., Wei, H. and Xu, H. X., "Remote excitation and remote detection of single quantum dot using propagating surface plasmons on silver nanowire," Chin. Phys. B 23(9), 097302 (2014).
[29] Neuhauser, R. G., Shimizu, K. T., Woo, W. K., Empedocles, S. A. and Bawendi, M. G., "Correlation between fluorescence intermittency and spectral diffusion in single semiconductor quantum dots," Phys. Rev. Lett. 85(15), 3301-3304 (2000).

[30] Galland, C., Ghosh, Y., Steinbruck, A., Sykora, M., Hollingsworth, J. A., Klimov, V. I. and Htoon, H., "Two types of luminescence blinking revealed by spectroelectrochemistry of single quantum dots," Nature 479(7372), 203-207 (2011).
[31] Chang, D. E., Sorensen, A. S., Hemmer, P. R. and Lukin, M. D., "Quantum optics with surface plasmons," Phys. Rev. Lett. 97(5), 053002 (2006).
[32] Li, Q., Wei, H. and Xu, H. X., "Resolving single plasmons generated by multiquantum-emitters on a silver nanowire," Nano Lett. 14(6), 3358-3363 (2014).
[33] Stranahan, S. M. and Willets, K. A., "Super-resolution Optical Imaging of Single-Molecule SERS Hot Spots," Nano Lett. 10(9), 3777-3784 (2010).
[34] Smith, C. S., Joseph, N., Rieger, B. and Lidke, K. A., "Fast, single-molecule localization that achieves theoretically minimum uncertainty," Nat. Methods 7(5), 373-375 (2010).
[35] Mortensen, K. I., Churchman, L. S., Spudich, J. A. and Flyvbjerg, H., "Optimized localization analysis for single-molecule tracking and super-resolution microscopy," Nat. Methods 7(5), 377-381 (2010).
[36] Cang, H., Labno, A., Lu, C. G., Yin, X. B., Liu, M., Gladden, C., Liu, Y. M. and Zhang, X., "Probing the electromagnetic field of a 15-nanometre hotspot by single molecule imaging," Nature 469(7330), 385-388 (2011).
[37] Lounis, B., Bechtel, H. A., Gerion, D., Alivisatos, P. and Moerner, W. E., "Photon antibunching in single CdSe/ZnS quantum dot fluorescence," Chem. Phys. Lett. 329(5-6), 399-404 (2000).
[38] Gruber, C., Kusar, P., Hohenau, A. and Krenn, J. R., "Controlled addressing of quantum dots by nanowire plasmons," Appl. Phys. Lett. 100(23), 231102 (2012).